

# Triply Triggered Doxorubicin Release From Supramolecular Nanocontainers

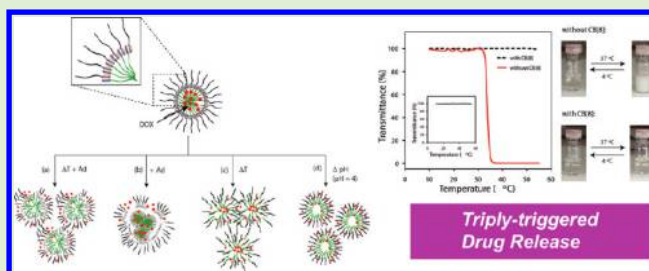
Xian Jun Loh,<sup>†</sup> Jesús del Barrio,<sup>†</sup> Pearl Pei Chern Toh,<sup>‡</sup> Tung-Chun Lee,<sup>†</sup> Dezhi Jiao,<sup>†</sup> Urs Rauwald,<sup>†</sup> Eric A. Appel,<sup>†</sup> and Oren A. Scherman<sup>\*,†</sup>

<sup>†</sup>Melville Laboratory for Polymer Synthesis, Department of Chemistry, University of Cambridge, Lensfield Road, Cambridge CB2 1EW, United Kingdom

<sup>‡</sup>Department of Medical Genetics, University of Cambridge, Cambridge Institute for Medical Research, Addenbrooke's Hospital, Hills Road, Cambridge CB2 0XY, United Kingdom

**S** Supporting Information

**ABSTRACT:** The synthesis of a supramolecular double hydrophilic block copolymer (DHBC) held together by cucurbit[8]uril (CB[8]) ternary complexation and its subsequent self-assembly into micelles is described. This system is responsive to multiple external triggers including temperature, pH and the addition of a competitive guest. The supramolecular block copolymer assembly consists of poly(*N*-isopropylacrylamide) (PNIPAAm) as a thermoresponsive block and poly(dimethylaminoethylmethacrylate) (PDMAEMA) as a pH-responsive block. Moreover, encapsulation and controlled drug release was demonstrated with this system using the chemotherapeutic drug doxorubicin (DOX). This triple stimuli-responsive DHBC micelle system represents an evolution over conventional double stimuli-responsive covalent diblock copolymer systems and displayed a significant reduction in the viability of HeLa cells upon triggered release of DOX from the supramolecular micellar nanocontainers.



## INTRODUCTION

Amphiphilic block copolymers undergo self-assembly into compartmentalized structures such as micelles or vesicles in aqueous media. Spherical micelles have been used in a variety of applications including pollutant extracting agents for the purification of wastewater,<sup>1</sup> templating agents for materials synthesis,<sup>2</sup> nanobioreactors for biologically relevant processes,<sup>3</sup> and as phase-transfer catalysts.<sup>4</sup> In recent years, however, these systems have been extensively investigated for their potential biomedical applications.<sup>5</sup> Micellar constructs with hydrophobic cores and hydrophilic coronas can aid in the aqueous solubilization of hydrophobic compounds, acting as nanocontainers.<sup>6</sup>

For drug-delivery applications, the micelles should remain stable and not rupture under sudden high dilution upon injection into the body. Therefore, micelles for such applications must have a low critical micelle concentration (CMC). One way to achieve a low CMC is to employ amphiphilic copolymers with an extremely hydrophobic segment to stabilize the micelle core. Unfortunately, this increased stability leads to incomplete drug release from the core.<sup>7</sup> To minimize the amount of drug introduced into the body, a complete and fully controlled drug release profile is required. Thus, a micellar delivery system that undergoes total disassembly with a specific stimulus and achieves complete drug release is highly desirable. Moreover, for total disassembly to occur, the micellar components must remain well solvated.

To this end, double hydrophilic block copolymers (DHBCs) that consist of two water-soluble blocks differing in chemical nature, have been prepared. These blocks must be designed with stimuli responsive capabilities. When an appropriate trigger such as pH or temperature is applied to these systems, DHBCs can reversibly self-assemble into micelle-like structures.<sup>8</sup> Through the application of these triggers, the hydrophilicity of the responsive block can be manipulated, allowing for tunable release of a drug encapsulated within the core.

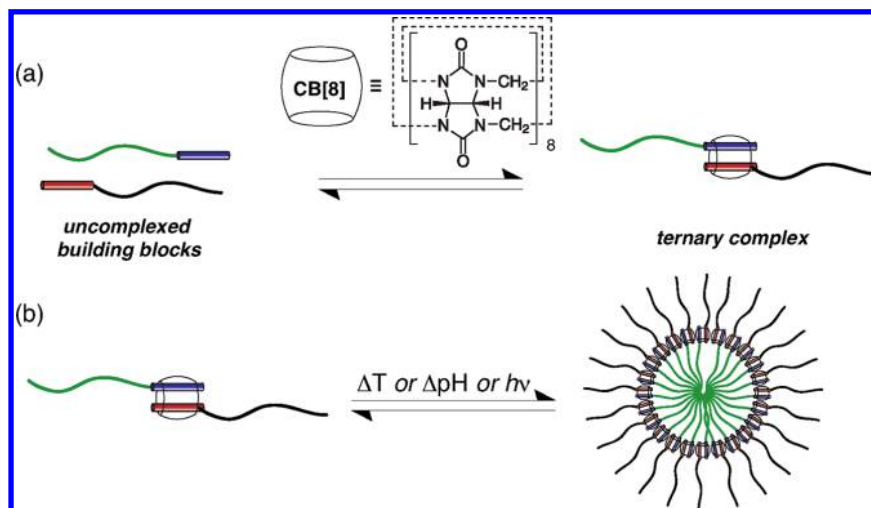
Herein we exploit the ability of cucurbit[8]uril (CB[8]) to simultaneously bind two guest molecules tethered to the chain ends of polymers in the construction of supramolecular DHBCs through a dynamic “handcuff”, as illustrated in Scheme 1.<sup>9</sup> CB[8] is a water-soluble macrocyclic host that has a cavity volume of 479 Å<sup>3</sup> and stabilizes ternary complexes consisting of electron-deficient and electron-rich aromatic motifs.<sup>10</sup> The highly tunable ternary nature of the CB[8] system along with its high binding constants in water ( $K_a \geq 10^{14} \text{ M}^{-2}$ ) make it particularly attractive for the construction of aqueous-based materials via a noncovalent route.<sup>11</sup> This supramolecular approach offers versatility and simplicity in the preparation of DHBCs as compared to conventional covalent techniques for polymer synthesis. In addition to conventional stimuli, such as

Received: August 19, 2011

Revised: December 12, 2011

Published: December 13, 2011

Scheme 1. (a) Formation of CB[8] Ternary Complex and (b) Subsequent Assembly into a Micellar Superstructure



temperature and pH, the use of CB[8] offers a new dimension to the stimuli-responsive nature of DHBCs by locking the two different polymer chains together in a noncovalent manner, as this linkage can be easily unlocked by the addition of a chemical stimuli as well.

A CB[8]-containing supramolecular DHBC was designed with poly(dimethylaminoethylmethacrylate) (PDMAEMA) as a pH-responsive segment and poly(*N*-isopropylacrylamide) (PNIPAAm) as a temperature-responsive block. Nanocontainers that are pH-responsive can be used for triggered release within endosomal and lysosomal vesicles at an acidic pH of 4, whereas temperature-responsive nanocontainers are suitable for triggering via remote heating methods such as infrared irradiation.<sup>12</sup> The molecular weights of the PDMAEMA ( $M_n \sim 9000$  g/mol) and PNIPAAm ( $M_n \sim 4000$  g/mol) polymers were restricted to below 10000 g/mol so that these segments can be readily excreted via renal filtration after use.<sup>13</sup> Herein, the design of a new class of systems for stimuli-responsive drug delivery and its potential chemotherapeutic application is described.

## EXPERIMENTAL SECTION

**Materials.** All starting materials were purchased from Alfa Aesar or Sigma Aldrich and were used as received unless stated otherwise. *N*-isopropylacrylamide (NIPAM) was recrystallized twice from hexane. CB[8] were prepared as documented previously.<sup>10</sup>

**Instrumentation.** <sup>1</sup>H NMR (400 MHz) spectra were recorded on a Bruker Avance QNP 400. UV/vis spectra were recorded on a Varian Cary 100 Bio UV-vis spectrophotometer. Dynamic light scattering (DLS) measurements were performed on Malvern Zetasizer NS90 instrument. Determination of solution binding constants were performed by ITC. Titration experiments were carried out on a VPITC from Microcal Inc., at 25 °C in 10 mM sodium phosphate buffer (pH = 7). The solution was degassed prior to titration, and 20–30 consecutive injections of 10–15 μL each were used, whereby the first injection was chosen to be 2 μL. Thus, the first data point was removed from the data set prior to curve fitting. Heats of dilution were checked by titration into the buffer solution and were found to be negligible in all cases. The data was analyzed with Origin 7.0 software, using the one set of sites model. A Zeiss Axiovert 200 M microscope with a LSM510 confocal attachment (63× NA 1.4 Plan-Apochromat oil-immersion lens LSM510 META, Carl Zeiss) along with the LSM510 version 3.2 software (Carl Zeiss) was used for fluorescent confocal microscopy.

**Synthesis of Naphthalene-Terminated Macroinitiator (Nap-Br) for ATRP.** 2-Naphthol (1 g, 6.9 mmol) was dissolved in 10 mL of anhydrous methylene chloride containing 7 mmol triethylamine in a 100 mL round-bottomed flask. The reaction flask was kept in an ice/water bath (temperature = 4 °C). When the 2-naphthol had completely dissolved, 7 mmol 2-bromoisobutryl bromide was added to the flask dropwise through an equalizing funnel. After addition, the reaction was allowed to proceed at room temperature for 24 h. Upon completion of the reaction, the white precipitate was filtered off. The resulting bromide-terminated ATRP initiator was obtained by extraction with 50 mL of deionized water three times. The yield of this reaction was about 64%.

**Synthesis of Naphthalene-Terminated Poly(dimethylaminoethylmethacrylate) (PDMAEMA).** The naphthalene-terminated PDMAEMA was synthesized by ATRP. A molar feed ratio of [DMAEMA (5 g)]/[Nap-Br (0.1 g, 0.34 mmol)]/[CuBr (98 mg)]/[HMTETA (315 mg)] of 93:1:2:4 was used. The reaction was performed in a 20 mL flask equipped with a magnetic stirrer. DMAEMA, Nap-Br, and HMTETA were introduced to the flask containing 15 mL of THF. After the reactants had completely dissolved, the reaction mixture was degassed by bubbling nitrogen through the reaction mixture for 30 min. CuBr was added to the reaction mixture under a nitrogen atmosphere. The reaction mixture was further purged with nitrogen for 10 min. The flask was then sealed and kept under a nitrogen atmosphere. The polymerization was allowed to proceed under continuous stirring at 45 °C for 24 h. The reaction was stopped by dilution with THF and being exposed to air for 4 h. The catalyst complex was removed by passing the dilute polymer solution through a short aluminum oxide column. A colorless solution was obtained. After the removal of THF under reduced pressure, the crude copolymer was redissolved in a minimum amount of THF and precipitated in hexane to remove the unreacted DMAEMA monomer. The obtained precipitate was dissolved in THF and then reprecipitated in diethylether. The polymer was dried in vacuo for further studies. The polymer yield after purification was 54.3%.

**Synthesis of the Hydroxyl Group Functionalized Chain Transfer Agent, CTA-OH.** The hydroxyl group containing CTA-OH (Scheme S1) was synthesized in the following manner. Ethanethiol (2.00 g, 32.19 mmol) was added to a stirred suspension of potassium phosphate (7.20 g, 33.92 mmol) in acetone (50 mL), and the reaction was stirred at room temperature for 45 min. Carbon disulfide (7.35 g, 96.53 mmol) was added, and the resulting bright yellow solution was further stirred for 45 min. Then, 4-(chloromethyl)benzyl alcohol (5.04 g, 32.18 mmol) was added, and the reaction mixture was left to stir at room temperature for 16 h. The reaction mixture was filtered and the volatiles were removed under reduced pressure. The solid residue was dissolved in ethyl acetate and the solution was subsequently washed

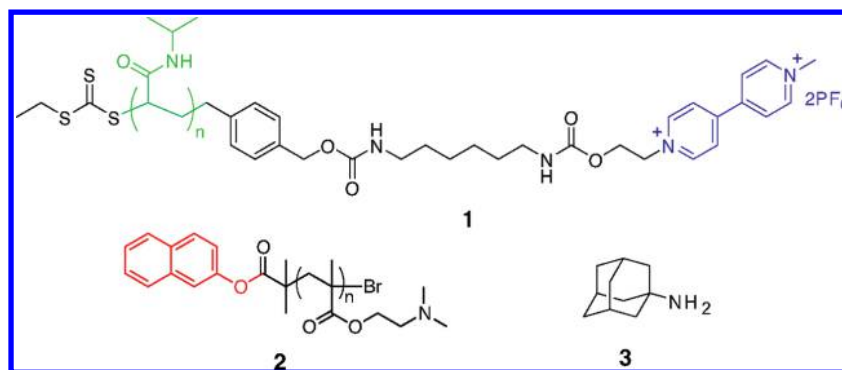


Figure 1. Chemical structures of the end-functionalized PNIPAAm 1, PDMAEMA 2, and adamantaneamine (Ad) 3.

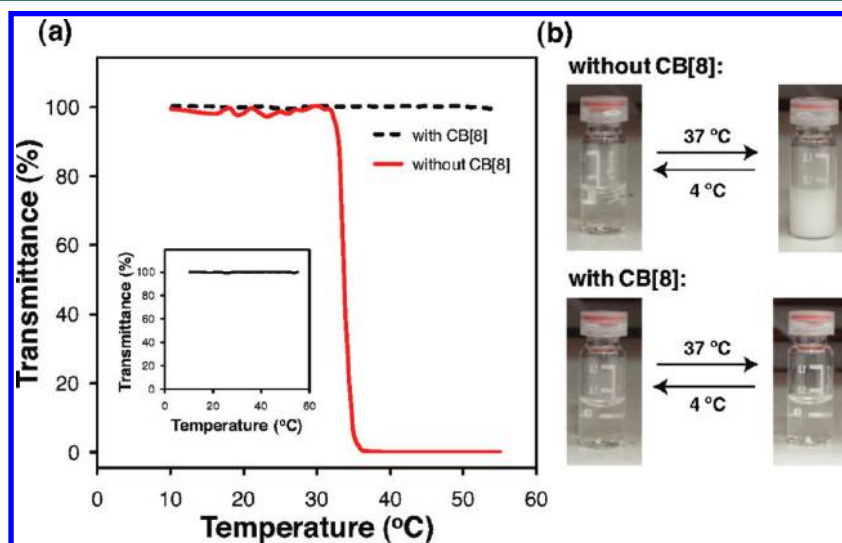


Figure 2. (a) Thermoresponsive behavior of **1** + **2** and **1** + **2** C CB[8] complex (0.25 mM) (inset shows the thermoresponsive behavior of the covalent micelle). (b) Photographs showing the effect of adding CB[8] to **1** + **2** mixtures.

with water and brine. The organic phase was dried over sodium sulfate and filtered. Then the solvent was evaporated and the crude product was purified by column chromatography using dichloromethane as eluent to give CTA-OH as yellow oil (6.24 g, 75%).  $^1\text{H NMR}$  (400 MHz,  $\text{CDCl}_3$ ): 7.30 (m, 4H), 4.67 (s, 2H), 4.61 (s, 2H), 3.38 (q,  $J = 7.4$  Hz, 2H), 1.36 (t,  $J = 7.4$  Hz, 2H).

**Synthesis of Hydroxyl Group Terminated Poly(*N*-isopropyl acrylamide), PNIPAM-OH.** *N*-Isopropyl acrylamide (1.500 g, 13.256 mmol), CTA-OH (0.137 g, 0.530 mmol), and ACPA (0.015 g, 0.054 mmol) were dissolved in 1,4-dioxane (6.6 mL) in a Schlenk tube, and the solution was degassed by bubbling nitrogen for 40 min. The Schlenk tube was then sealed and heated in an oil bath set to 70 °C for 7 h. Upon completion, the polymerization mixture was cooled in liquid nitrogen and the polymer was isolated by precipitation from cold diethyl ether. The resulting polymer was collected via decanting off the solution, dissolving the remaining polymer in tetrahydrofuran, and then removing the solvent under reduced pressure. PNIPAM-OH was obtained as a waxy yellow solid. Yield: 1.457 g (89%).  $^1\text{H NMR}$  (400 MHz,  $\text{CDCl}_3$ ): 7.22–7.33 (br), 7.06–7.17 (m, 2H), 5.91–7.01 (br), 4.63 (s, 2H), 3.83–4.16 (br, 25H), 3.27–3.39 (m, 2H), 1.20–2.34 (br, 78H), 0.95–1.20 (br, 150H).  $M_n(\text{NMR}) = 3100$  g/mol,  $M_n(\text{GPC}) = 2900$  g/mol,  $M_w/M_n = 1.35$ .

**Synthesis of Methylviologen Terminated Poly(*N*-isopropyl acrylamide), PNIPAM-MV.** PNIPAM-OH (0.183 g, 0.059 mmol) was added to a solution of MV-NCO (0.120 g, 0.178 mmol) in dry acetonitrile (5 mL). After addition of a drop of dibutyltin dilaurate, the resulting solution was stirred for 48 h at room temperature. The solvent was partially evaporated under reduced pressure, and the crude product was obtained by precipitation from cold diethylether. Then, the crude product was washed with tetrahydrofuran and the washing solvent was

collected. Finally, the solvent was evaporated under reduced pressure to give PNIPAM-MV as a yellow powder. Yield: 0.168 g (75%).  $^1\text{H NMR}$  (400 MHz, DMSO): 9.34 (d,  $J = 6.8$  Hz, 2H), 9.29 (d,  $J = 6.8$  Hz, 2H), 8.79 (d,  $J = 6.8$  Hz, 2H), 8.75 (d,  $J = 6.8$  Hz, 2H), 6.88–7.63 (m, 25H), 4.91–4.99 (m, 4H), 4.39–4.55 (m, 5H), 3.72–3.96 (m, 25H), 3.30 (br), 2.84–2.98 (m, 4H), 1.78–2.16 (br, 78H), 0.90–1.70 (br, 150H).  $M_n(\text{NMR}) = 3800$  g/mol,  $M_n(\text{GPC}) = 3600$  g/mol,  $M_w/M_n = 1.40$ .

**Preparation and Characterization of DOX-Loaded Micelles.** DOX-loaded micelle formulations were prepared by a solvent evaporation method. DOX-HCl was solubilized in THF (2.5 mg/mL) containing triethylamine (6 M equiv to DOX) followed by 10 min sonication, and subsequently added dropwise to a stirring aqueous suspension of **1** + **2** C CB[8] complex micelles (10 mg/mL) at 4 °C. The mixture was kept under magnetic stirring overnight in the dark at 40 °C in an open atmosphere to evaporate the THF. Aggregates were removed by centrifugation, and unincorporated DOX in the supernatant was removed by dialysis (MWCO 100 kDa). The purified DOX-loaded micelles were collected by freeze-drying. The drug loading efficiency was calculated by weighing the lyophilized micelles and dissolving in dimethyl sulfoxide (DMSO). This causes complete dissolution of the micelle and release of the encapsulated DOX. Particulate matter from the supramolecular complex was removed by centrifugation. Unloaded micelles were used as the blank sample. The amount of entrapped DOX was determined by measuring the UV absorbance at 480 nm of the drug-loaded polymeric micelles dissolved in DMSO. DOX content was expressed as the weight ratio between loaded DOX and total weight of DOX-loaded micelle, and loading efficiency as the weight percent of encapsulated DOX to total feeding



DOX. The loading efficiency of DOX in the micelles was 18%. All loading measurements were performed in triplicate.

**Release Study of DOX-Loaded Micelles.** The release profile of DOX from DOX-loaded micelles was determined by dialysis. DOX-micelle (1 mg/mL DOX-micelle containing 45  $\mu$ g DOX) was loaded into MWCO 100 kDa dialysis tubing and dialyzed against 7 mL of phosphate buffered saline (PBS, pH 7.4) in the dark at 37 °C. At specified time points, 1 mL of the dialysis buffer was collected and replaced with equal volume of fresh PBS. The concentrations of DOX present in the dialysate were determined by measuring absorbance at 480 nm. The concentration of DOX released from the micelles was expressed as a percentage of the total DOX and plotted as a function of time.

**Cell Culture.** HeLa, human cervical carcinoma cells, were cultivated in DMEM containing 10% fetal bovine serum (FBS) and 1% penicillin/streptomycin. Cells grew as a monolayer and were passaged upon confluence using trypsin (0.5% w/v in PBS). The cells were harvested from culture by incubating in trypsin solution for 15 min. The cells were centrifuged, and the supernatant was discarded. A 3 mL portion of serum-supplemented DMEM was added to neutralize any residual trypsin. The cells were resuspended in serum-supplemented DMEM at a concentration of  $2 \times 10^4$  cells/mL. Cells were cultivated at 37 °C and 5% CO<sub>2</sub>.

**Intracellular Release of DOX.** The cellular uptake and intracellular release behavior of the DOX-loaded supramolecular micelles were followed with confocal laser scanning microscopy (CLSM) using HeLa cells. HeLa cells were cultured on a coverslip containing 2 mL of DMEM for 2 days to 70% confluency. The cells were incubated with DOX-loaded supramolecular micelles or free DOX for 4 h at 37 °C in a humidified 5% CO<sub>2</sub>-containing atmosphere. The culture media were removed and the cells were rinsed two times with PBS prior to the fluorescence observation. All confocal images were taken with a 63 $\times$  oil-immersion lens. Microscopy was performed on cells which have been fixed in 4% paraformaldehyde for 20 min on coverslips. Coverslips were mounted in Prolong Gold Antifade reagent with 4',6-diamidino-2-phenylindole (DAPI; Molecular Probes, Invitrogen).

**Evaluation of Cytotoxicity.** The cytotoxicity of DOX-incorporated micelles against HeLa cells was determined by MTT assay in a 96-well cell culture plate. All copolymer solutions were sterilized by filtration with a 0.45  $\mu$ m filter before tests. HeLa cells were seeded at a density of  $1 \times 10^4$  cells/well in a 96-well plate, and incubated for 24 h. Cells were then incubated with fresh serum-free DMEM containing free DOX, DOX-loaded micelles, and unloaded micelles at various concentrations for 2 h. Cells were rinsed with PBS twice, and 100  $\mu$ L of growth media was added and incubated for another 48 h. Following that, 10 mL of 3-(4,5-dimethylthiazol-2-yl)-2,5-diphenyl tetrazolium bromide (MTT) solution (5 mg/mL) was added to each well. After 4 h of incubation at 37 °C, the MTT solution was removed, and the insoluble formazan crystals that formed were dissolved in 100  $\mu$ L of dimethylsulfoxide (DMSO). The absorbance of the formazan product was measured at 570 nm using a spectrophotometer. Untreated cells in media were used as a control. All experiments were carried out with six replicates.

**Statistical Analysis.** Data are expressed as mean standard deviation (SD). Analysis of variance (ANOVA), followed by Student's *t*-test, was used to determine the significant differences among the groups, and *p*-values less than 0.05 were considered significant.

## RESULTS AND DISCUSSION

**Preparation of Supramolecular Micelles.** Methylviologen-terminated PNIPAAm (**1**) was synthesized through a postpolymerization procedure involving a PNIPAAm polymer containing a hydroxyl group in one chain end and a methylviologen having an isocyanate group. In addition, a naphthalene-terminated PDMAEMA (**2**) was prepared via atom-transfer radical polymerization (ATRP) from the requisite functional initiators, and their structures are shown in Figure 1. A covalent DHBC, PDMAEMA<sub>60</sub>-*b*-PNIPAAm<sub>35</sub>, was prepared

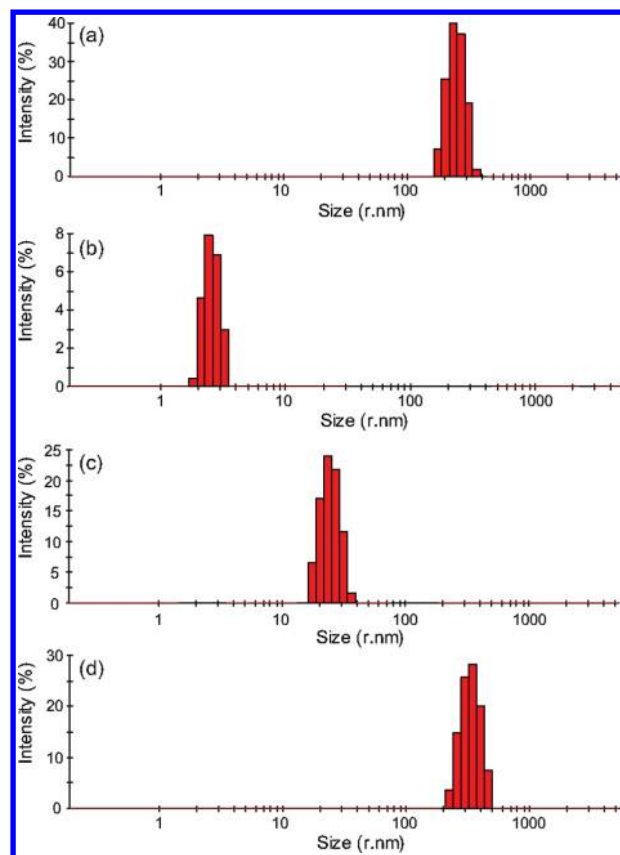


**Figure 3.** Particle size distributions of micelles after being exposed to various stimuli: (a) no trigger, (b) temperature trigger, (c) adamantaneamine trigger, (d) pH trigger (solution concentration = 50  $\mu$ M).

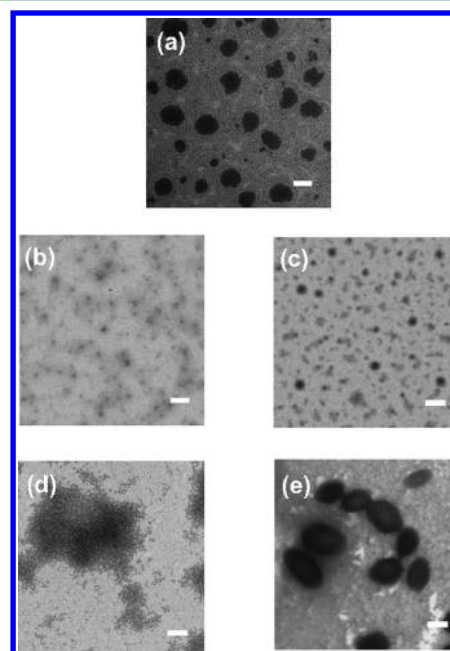


**Figure 4.** TEM micrographs of micelles after being exposed to various stimuli: (a) no trigger, (b) temperature + adamantaneamine trigger, (c) temperature trigger, (d) adamantaneamine trigger, and (e) pH trigger (scale bar denotes 200 nm, solution concentration = 250  $\mu$ M).

as a control by sequential ATRP polymerization of the corresponding monomers. As CB[8] is able to simultaneously

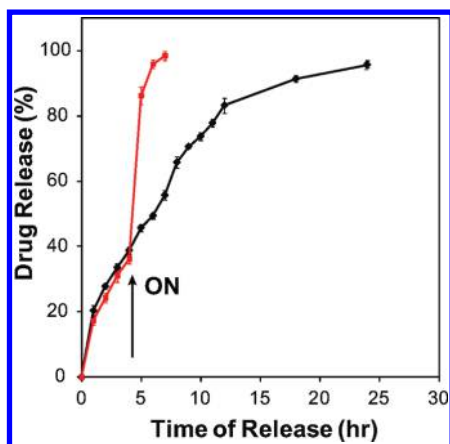


**Figure 5.** (a) Drug release profile from the supramolecular micelles made from **1** + **2** + CB[8] complex. The red line represents the profile obtained after the system was exposed to the combined adamantane and temperature triggers, while the black line represents the profile obtained without any triggers.

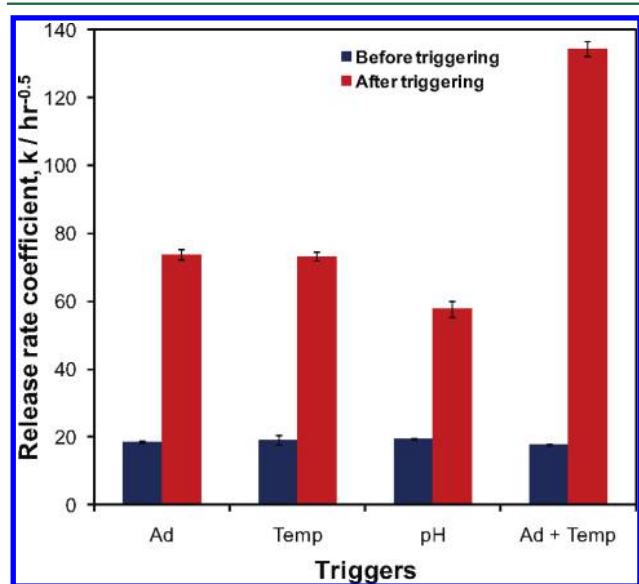


**Figure 6.** Release rate coefficients of the systems after exposure to various triggers.

bind two guests forming a 1:1:1 ternary complex, **1**, **2**, and CB[8] were mixed in a equimolar ratio in aqueous solution.

Formation of the ternary complex was confirmed by several characterization methods including <sup>1</sup>H NMR spectrometry, UV/vis spectroscopy, and isothermal titration calorimetry (ITC).<sup>9</sup> The solution containing **1** + **2** + CB[8] displayed an upfield shift in the <sup>1</sup>H NMR as well as broadening of the peaks corresponding to the naphthalene moiety on the chain end of the PDMAEMA (Figure S1), while a solution of **1** and **2** alone did not differ from the individual component spectra. UV/vis spectra of **1**, **2**, and CB[8] showed a significant charge-transfer band with a peak at 550 nm in line with previous reports.<sup>9</sup> However, UV/vis spectra of solutions containing either **1** or **2** did not show appreciable absorption beyond 500 nm (Figure S2). In addition, ITC measurements were performed to establish a solution binding constant of  $1.34 \times 10^4 \text{ M}^{-1}$  for the second binding equilibrium arising from **1** + CB[8] with **2** (Figure S3). These results together offer compelling evidence that homopolymer chains **1** and **2** can indeed be linked

together using CB[8] to form the supramolecular DHBC, as depicted in Scheme 1a.

**Solution Properties of Supramolecular Micelles.** The difference observed in the solution properties of the mixture of homopolymers **1** and **2** with and without CB[8] is remarkable (Figure 2). In the absence of CB[8], the aqueous mixture of **1** and **2** shows the usual phase transition typical of PNIPAAm both above and below its lower critical solution temperature (LCST). When the temperature is 4 °C, small particles were detected by dynamic light scattering (DLS) while the solution appeared transparent. Above the LCST of 35 °C, large micrometer-sized particles are detected, resulting in a turbid solution as clearly seen in the transmittance measurements shown in Figure 2a. Upon addition of CB[8] to the polymer mixture in water, the solution remains transparent, even as the temperature is raised above the LCST of PNIPAAm. The particle size observed by DLS at 4 °C is <10 nm, corresponding to unimers, while at temperatures above the LCST, the particle size increases to 280 nm, indicating the self-assembly of compartmentalized superstructures, as shown in Figure 3. Such a superstructure has been previously reported to form on account of the aggregation of micelles.<sup>14</sup>

To investigate the self-assembly behavior of the supramolecular micelles, the critical micelle concentration (CMC) in water was determined by investigating the scattering intensity of light as a function of the supramolecular DHBC concentration. An abrupt increase in the scattering intensity was observed when the polymer concentration was above a certain value, which corresponds to the CMC (Figure S4).<sup>15</sup> The CMC values for both the supramolecular micelle and its covalent analogue were estimated to be 20 and 32 μM, respectively. The CMC value of the supramolecular micelle determined in a 1× PBS solution containing 1% fetal bovine serum at 37 °C was about 14 μM. After an additional 3 days of incubation, the CMC value remains largely unchanged (see Figure S5). This result shows that the system is stable under physiological conditions. When the micelles were titrated with a competitive guest for the CB[8] cavity, such as adamantane-amine **3**, the particle size was observed to decrease drastically to only 20 nm (Figure 3). On the other hand, when the neutral pH was lowered to a value of 4, the particle size increased from 280 nm to roughly 340 nm (Figure 3). This could be on account of the increased protonation along the PDMAEMA backbone (corona) and subsequent repulsion of the charged segments, leading to an increase in the particle size.<sup>16</sup> These DLS measurements corroborate with the images obtained using transmission electron microscopy (Figure 4).

**In Vitro Cytotoxicity.** As these supramolecular micelles were shown to be highly responsive to external environmental stimuli, they were loaded with the drug doxorubicin (DOX) and tested for stimuli-triggered anticancer activity. DOX is an anthracycline antibiotic widely used in cancer chemotherapy for the treatment of a broad range of cancers, including hematological malignancies, many types of carcinoma, and soft tissue sarcomas. It has been used in many micelle drug release studies as a model drug.<sup>17</sup> Its major drawback, however, is its high toxicity, which leads to critical side effects in clinical applications. The drug was incorporated into the micelles by a standard solvent exchange and dialysis protocol. Previous work on micelles containing PNIPAAm as the hydrophobic domain have suggested that DOX is loaded into the micelle core.<sup>18</sup> The drug release profiles of both the supramolecular and covalent

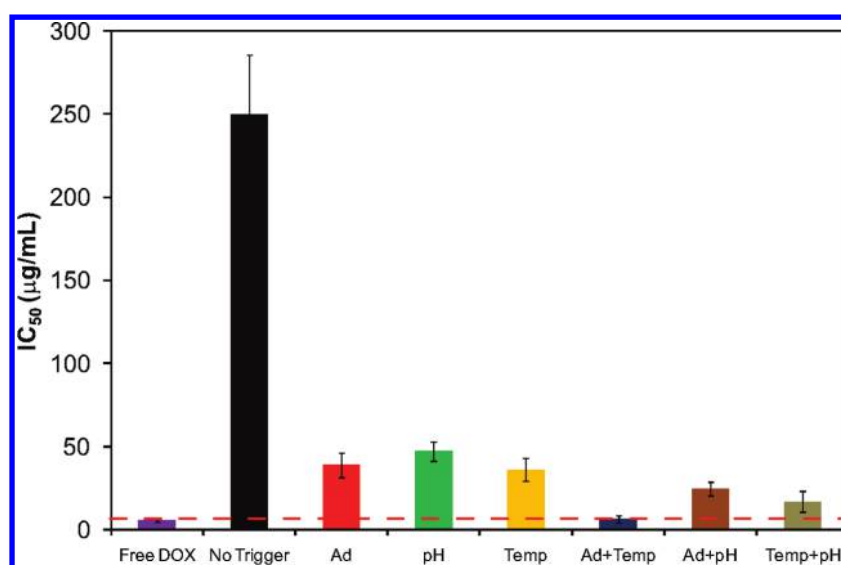
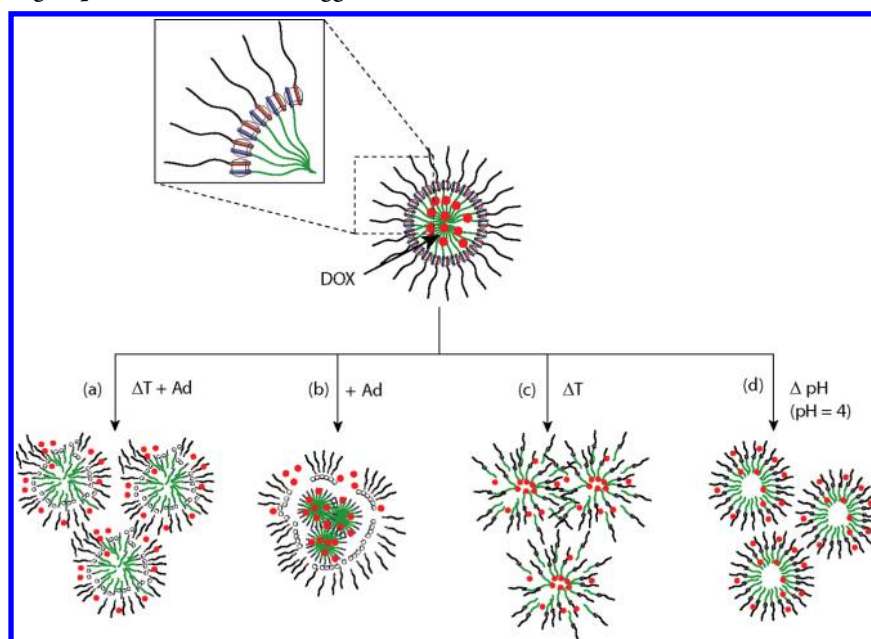


Figure 7. IC<sub>50</sub> values of the drug/micelle formulation (under different stimuli) after being exposed to HeLa cells for 2 h.

**Scheme 2. Hierarchical Self Assembly of the Supramolecular Entity under Different Conditions and Its Subsequent Mode of Drug Release after Being Exposed to Different Triggers**



DHBC micelles are shown in Figure 5 and Figure S6, respectively.

In the absence of any stimulus, the drug release profiles for both covalent and supramolecular micelles appear to obey the  $(M_t)/(M_\infty) = k \cdot t^n$  equation, where  $M_t$  and  $M_\infty$  are the mass of drug released at time  $t$  and infinite time, respectively,  $k$ , a characteristic exponent of the mode of transport of the drug, and  $n = 0.5$ , assuming drug release obeys a Fickian diffusional profile.<sup>19</sup> The value of  $k$  incorporates the diffusional coefficient of the drug from the system and its magnitude gives an indication of the rate of release of the drug from the micelles. To trigger the release of the drug, three different forms of triggers can be used. First, a temperature stimulus of lowering the temperature from 37 to 15 °C will cause the hydrophobic PNIPAAm core to solubilize and release the drug content in the core. Using the site-specific delivery requires the use of a

remote trigger (temperature) to tune the exact rupture of the micelles. This allows the drug to be released at exactly the right time and place. Local thermotherapy at the target site, using microwave, ultrasound, or infrared irradiation could be used to trigger the nanoparticle release.<sup>20</sup> Second, the lowering of the pH from 7 to 4 will protonate the amino group in the PDMAEMA segment, and this will cause the micelle to swell and enhance the rate of DOX release. pH-sensitive polymeric carriers have been used in targeted antitumor drug delivery.<sup>21</sup> This approach is based on the intrinsic pH differences between various solid tumors and the surrounding normal tissues.<sup>22</sup> Third, the addition of a competitive guest such as adamantane-amine will disrupt the ternary complex that is formed and cause the rupture of the micelle superstructure. A solution of adamantane-amine or proteins functionalized with adamantane can be applied directly to the tumor site after the application of



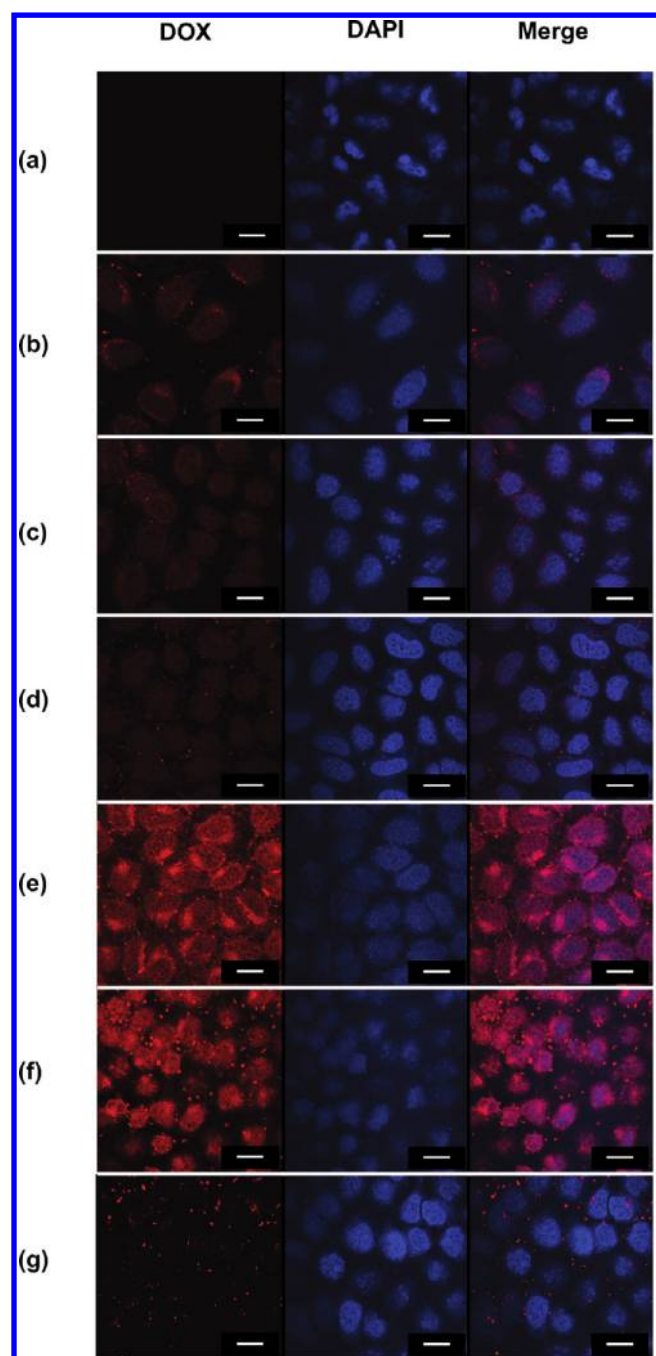


**Figure 8.** CLSM images of HeLa cells incubated with supramolecular micelles under different conditions: (a) control (without micelles), (b) temperature trigger, (c) adamantaneamine trigger, (d) pH trigger, (e) free DOX, (f) combined temperature and adamantaneamine triggers, and (g) no trigger (scale bar denotes 20  $\mu\text{m}$ , solution concentration of loaded micelle = 500  $\mu\text{g}/\text{mL}$ ).

the micelle solution. This type of directed delivery leads to the release of the drug at the local site. Other stimuli-responsive polymers based on PNIPAAm do not have such multistimuli capabilities.<sup>18</sup> These supramolecular micelles have a faster release rate than the covalent micelles, showing that the dynamic noncovalent system does not encapsulate the drug as tightly as their covalent counterparts. This could be due to the difference in the stability of the noncovalent system compared to the covalent system.

When different triggers were applied, the rate of release was accelerated. The manipulation of pH, temperature or the addition of competitive guest 3 all increased the release rate of the supramolecular micelles by more than three times (Figure 6) ( $p < 0.05$ ). A similar observation was found for the covalent micelles, although there was no such effect when 3 was added to this system. The ability to manipulate the release profile at a specific time or location in the body remains a definitive challenge for every stimuli-responsive drug delivery vehicle. To this end, a “burst” release effect was realized for the DOX-loaded supramolecular DHBC micelles using the combined triggers of temperature and a competitive guest for CB[8], thereby ensuring total and complete drug release at a specific time as evident in Figure 5. This combined external trigger was much more effective than any stimulus alone, which highlights a major advantage of using the supramolecular DHBC micelles over their covalent analogues ( $p < 0.05$ ).

To demonstrate the potential utility of the supramolecular DHBC micelles, DOX-loaded micelles, unloaded micelles, and free DOX were exposed to HeLa cells for 2 h followed by a cell viability assessment using a 3-(4,5-dimethylthiazol-2-yl)-2,5-diphenyl tetrazolium bromide (MTT) assay. The  $\text{IC}_{50}$  (concentration for 50% cell death) of the DOX-loaded supramolecular micelles under different stimuli are shown in Figure 7. All the cell viability graphs from which the  $\text{IC}_{50}$ s were determined are shown in Figures S7–S17. Unloaded micelles, formed from both supramolecular or covalent systems, were well tolerated by the HeLa cells, at polymer concentrations of up to 1 mg/mL. The  $\text{IC}_{50}$  of free DOX and micelle-encapsulated DOX were calculated to be  $5.62 \pm 1.2$  and  $250.2 \pm 35.4$   $\mu\text{g}/\text{mL}$  DOX, respectively. We note that the higher  $\text{IC}_{50}$  of micellar DOX is observed as a result of the slower rate of DOX release from DOX-loaded micelles, in accordance with previous reports.<sup>23</sup>

The  $\text{IC}_{50}$  of the drug-loaded micelle can be tuned by the use of three stimuli: pH, temperature, and the addition of a competitive CB[8] guest. The application of a pH stimulus reduced the  $\text{IC}_{50}$  to  $47.1 \pm 5.6$   $\mu\text{g}/\text{mL}$ , while the lowering of the temperature from 37 to 15  $^{\circ}\text{C}$  resulted in a reduction of the  $\text{IC}_{50}$  to  $36.1 \pm 6.9$   $\mu\text{g}/\text{mL}$ . Similarly, the addition of adamantaneamine 3 reduced the  $\text{IC}_{50}$  to  $38.9 \pm 7.6$   $\mu\text{g}/\text{mL}$ . The addition of adamantaneamine along with a change in pH reduced the  $\text{IC}_{50}$  to  $24.54 \pm 4.3$   $\mu\text{g}/\text{mL}$ . The lowering of temperature along with a change in pH reduced the  $\text{IC}_{50}$  to  $16.78 \pm 6.2$   $\mu\text{g}/\text{mL}$ . Finally, the combined use of temperature along with addition of a competitive guest dramatically reduced the  $\text{IC}_{50}$  to  $6.38 \pm 2.2$   $\mu\text{g}/\text{mL}$ , which is roughly the value of free DOX. Exposing the supramolecular system to different stimuli increased the rate of drug release ( $p < 0.05$ ). This is likely caused by the change in the micelle structure as shown in Scheme 2. When a faster rate of DOX release is achieved, the  $\text{IC}_{50}$  of the DOX-loaded micelles decreased as a result of the enhanced toxicity. Therefore, we have shown that the supramolecular micelle system was able to (1) reduce the toxicity of DOX upon incubation with HeLa cells and (2) induce toxicity as and when desired via the use of a local and remote stimulus in a combined “burst” approach. In contrast, the covalent analogue was only responsive to pH and temperature stimuli and represented a more limited option as compared to the supramolecular system.

**Intracellular Distribution of DOX-Loaded Supramolecular Micelles.** The uptake of DOX-loaded supramolecular micelles by HeLa cells was monitored by confocal laser

scanning microscopy (CLSM; Figure 8). The cell nuclei were stained blue by DAPI staining; DAPI is a fluorescent stain that binds strongly to A–T rich regions in DNA present in the cell nucleus. As shown in Figure 8, after a 4 h incubation of the HeLa cells with free DOX, a small amount of DOX was found in the cytoplasm of the cells. An overlay of the blue regions corresponding to the nuclei and the bright red fluorescence of DOX indicates that a large amount of the DOX had localized in the cell nuclei. In contrast, DOX released from the supramolecular micelles (without the effect of any triggers) showed poor uptake and accumulated largely within the cytoplasm. Upon exposure to either temperature, pH, or adamantaneamine triggers, a larger proportion of the released DOX was localized in the cell nuclei, attesting to the increased rate of release of DOX from the micelles. Finally, a combination of both temperature and adamantaneamine triggers resulted in a much greater accumulation of DOX (at levels comparable to that of free DOX) within the cell nuclei. This result shows that the encapsulation and triggered release of DOX from the supramolecular micelles allows for control over the release of the drug at a targeted site.

## CONCLUSIONS

In conclusion, we have demonstrated that supramolecular DHBC micelles readily self-assembled from ternary complexes consisting of end-functionalized PDMAEMA and PNIPAAm with CB[8] acting as a dynamic “handcuff”. A chemotherapeutic drug DOX could be easily encapsulated within the supramolecular micelles, thereby reducing systemic toxicity until the application of an external stimulus at a desired time, which is important for drug delivery in chemotherapy. Furthermore, a multitrigged “burst” release system was realized for the controlled reduction in the viability of human cervical carcinoma cells. We envision that this supramolecular DHBC system will lead to a new generation of stimuli-responsive drug delivery vehicles for intracellular delivery of a wide variety of biologically relevant molecules and stimulate the development of unique and clinically applicable therapies.

## ASSOCIATED CONTENT

### Supporting Information

Spectral characterization data, drug release profiles, and cell culture data. This material is available free of charge via the Internet at <http://pubs.acs.org>.

## AUTHOR INFORMATION

### Corresponding Author

\*E-mail: [oas23@cam.ac.uk](mailto:oas23@cam.ac.uk).

## ACKNOWLEDGMENTS

X.J.L. thanks A\*STAR for a Postdoctoral Fellowship and J.d.B. is grateful for a Marie Curie Intra-European Fellowship. This work was also supported by an ERC Starting Investigator Grant (ASPiRe) and a Next Generation Fellowship provided by Walters-Kundert Foundation. We like to thank Dr. Jeremy Skepper for his kind assistance with the TEM measurements.

## REFERENCES

- (1) Paria, S. *Adv. Colloid Interface Sci.* **2008**, *138*, 24–58.
- (2) Walker, L. M.; Kuntz, D. M. *Curr. Opin. Colloid Interface Sci.* **2007**, *12*, 101–105.
- (3) Wang, Z. L. *Appl. Microbiol. Biotechnol.* **2007**, *75*, 1–10.

- (4) Fiamegos, Y. C.; Stalikas, C. D. *Anal. Chim. Acta* **2005**, *550*, 1–12.
- (5) Kwon, G. S.; Kataoka, K. *Adv. Drug Delivery Rev.* **1995**, *16*, 295–309.
- (6) (a) Torchilin, V. P. *J. Controlled Release* **2001**, *73*, 137–172. (b) Loh, X. J.; Zhang, Z. X.; Wu, Y. L.; Lee, T. S.; Li, J. *Macromolecules* **2009**, *42*, 194–202.
- (7) (a) Li, Y. Y.; Zhang, X. Z.; Kim, G. C.; Cheng, H.; Cheng, S. X.; Zhuo, R. X. *Small* **2006**, *2*, 917–923. (b) Tang, Y. Q.; Liu, S. Y.; Armes, S. P.; Billingham, N. C. *Biomacromolecules* **2003**, *4*, 1636–1645.
- (8) Kabanov, A. V.; Kabanov, V. A. *Adv. Drug Delivery Rev.* **1998**, *30*, 49–60.
- (9) (a) Rauwald, U.; Scherman, O. A. *Angew. Chem., Int. Ed.* **2008**, *47*, 3950–3953. (b) Rauwald, U.; del Barrio, J.; Loh, X. J.; Scherman, O. A. *Chem. Commun.* **2011**, *47*, 6000–6002.
- (10) (a) Day, A.; Arnold, A. P.; Blanch, R. J.; Snushall, B. J. *Org. Chem.* **2001**, *66*, 8094–8100. (b) Kim, J.; Jung, I. S.; Kim, S. Y.; Lee, E.; Kang, J. K.; Sakamoto, S.; Yamaguchi, K.; Kim, K. *J. Am. Chem. Soc.* **2000**, *122*, 540–541. (c) Kim, H. J.; Heo, J.; Jeon, W. S.; Lee, E.; Kim, J.; Sakamoto, S.; Yamaguchi, K.; Kim, K. *Angew. Chem., Int. Ed.* **2001**, *40*, 1526. (d) Bush, M. E.; Bouley, N. D.; Urbach, A. R. *J. Am. Chem. Soc.* **2005**, *127*, 14511–14517. (e) Rauwald, U.; Biedermann, F.; Deroo, S.; Robinson, C. V.; Scherman, O. A. *J. Phys. Chem. B* **2010**, *114*, 8606–8615.
- (11) Geng, J.; Jiao, D. Z.; Rauwald, U.; Scherman, O. A. *Aust. J. Chem.* **2010**, *63*, 627–630.
- (12) (a) Duncan, R. *Nat. Rev. Cancer* **2006**, *6*, 688–701. (b) Duncan, R. *Biochem. Soc. Trans.* **2007**, *35*, 56–60. (c) Liu, T. Y.; Hu, S. H.; Liu, D. M.; Chen, S. Y.; Chen, I. W. *Nano Today* **2009**, *4*, 52–65.
- (13) (a) Yamaoka, T.; Tabata, Y.; Ikada, Y. *J. Pharm. Sci.* **1995**, *84*, 349–354. (b) Yamaoka, T.; Tabata, Y.; Ikada, Y. *J. Pharm. Sci.* **1994**, *83*, 601–606.
- (14) (a) Loh, X. J.; Wu, Y. L.; Seow, W. T. J.; Norimzan, M. N. I.; Zhang, Z. X.; Xu, F.; Kang, E. T.; Neoh, K. G.; Li, J. *Polymer* **2008**, *49*, 5084–5094. (b) Loh, X. J.; Cheong, W. C. D.; Li, J.; Ito, Y. *Soft Matter* **2009**, *5*, 2937–2946.
- (15) Joo, M. K.; Sohn, Y. S.; Jeong, B. *Macromolecules* **2007**, *40*, 5111–5115.
- (16) Bougard, F.; Jeusette, M.; Mespouille, L.; Dubois, P.; Lazzaroni, R. *Langmuir* **2007**, *23*, 2339–2345.
- (17) (a) Ahmed, F.; Discher, D. E. *J. Controlled Release* **2004**, *96*, 37–53. (b) Lee, E. S.; Na, K.; Bae, Y. H. *Nano Lett.* **2005**, *5*, 325–329. (c) Shuai, X. T.; Ai, H.; Nasongkla, N.; Kim, S.; Gao, J. M. *J. Controlled Release* **2004**, *98*, 415–426.
- (18) (a) Liu, S. Q.; Tong, Y. W.; Yang, Y. Y. *Biomaterials* **2005**, *26*, 5064–5074. (b) Lo, C. L.; Huang, C. K.; Lin, K. M.; Hsiue, G. H. *Biomaterials* **2007**, *28*, 1225–1235.
- (19) (a) Loh, X. J.; Deen, G. R.; Gan, Y. Y.; Gan, L. H. *J. Appl. Polym. Sci.* **2001**, *80*, 268–273. (b) Loh, X. J.; Goh, S. H.; Li, J. *Biomaterials* **2007**, *28*, 4113–4123. (c) Loh, X. J.; Vu, P. N. N.; Kuo, N. Y.; Li, J. *J. Mater. Chem.* **2011**, *21*, 2246–2254. (d) Loh, X. J.; Peh, P.; Liao, S.; Sng, C.; Li, J. *J. Controlled Release* **2010**, *143*, 175–182.
- (20) Liu, L.; Wang, W.; Ju, X. J.; Xie, R.; Chu, L. Y. *Soft Matter* **2010**, *6*, 3759–3763.
- (21) (a) Gillies, E. R.; Frechet, J. M. J. *Bioconjugate Chem.* **2005**, *16*, 361–368. (b) Bae, Y.; Nishiyama, N.; Fukushima, S.; Koyama, H.; Yasuhiro, M.; Kataoka, K. *Bioconjugate Chem.* **2005**, *16*, 122–130. (c) Lee, E. S.; Gao, Z. G.; Kim, D.; Park, K.; Kwon, I. C.; Bae, Y. H. *J. Controlled Release* **2008**, *129*, 228–236.
- (22) Leeper, D. B.; Engin, K.; Thistlethwaite, A. J.; Hitchon, H. D.; Dover, J. D.; Li, D. J.; Tupchong, L. *Int. J. Radiat. Oncol., Biol., Phys.* **1994**, *28*, 935–943.
- (23) Kim, T. H.; Mount, C. W.; Gombotz, W. R.; Pun, S. H. *Biomaterials* **2010**, *31*, 7386–7397.